# Curvature-Dependent Elastic Properties of Liquid-Ordered Domains Result in Inverted Domain Sorting on Uniaxially Compressed Vesicles

Risselada, H. Jelger; Marrink, Siewert Jan; Mueller, Marcus

*Published in:*
Physical Review Letters

*DOI:*
10.1103/PhysRevLett.106.148102



*Publication date:*
2011

# Supplemental Material: Curvature-dependent elastic properties of liquid-ordered domains result in inverted domain sorting on uni-axially compressed vesicles

H. Jelger Risselada[1], Siewert Jan Marrink[2], and Marcus Müller[3]
[1] *Theoretical Molecular Biophysics Group, Max-Planck-Institute for Biophysical Chemistry, 37077 Göttingen, Germany*
[2] *University of Groningen, Nijenborgh 4, 9747 AG Groningen, The Netherlands*
[3] *Institut für Theoretische Physik, Georg-August-Universität, 37077 Göttingen, Germany*
(Dated: March 28, 2011)

## SIMULATION MODEL AND SETUP

*Simulation model.* The simulations described in this paper were performed with the GROMACS simulation package[4], version 4.0.5. We used the MARTINI model version 2.1 [5] to simulate the lipids and cholesterol. The MARTINI model uses a 4-to-1 mapping; i.e., on average, 4 heavy atoms are represented by a single interaction center, with an exception for ring-like molecules such as cholesterol that are mapped with somewhat higher resolution (≈3-to-1). Solvent is explicitly included and four water molecules are modeled as a single bead. The interactions between the CG sites are modeled by a set of short-ranged Lennard-Jones potentials. Charged groups such as the zwitterionic lipid head groups also interact via a Coulombic energy function. Shifted potentials are used to describe both Lennard-Jones and electrostatic non-bonded pair-wise interactions. In both cases the neighbor list cutoff is 1.2 nm and these potentials are gradually shifted to zero when the pair-wise distance exceeded 0.9 nm. More specific details about the MARTINI model can be found in the original publication[5]. Details about the parameterizations of the lo/ld components are given in the supplementary material of our recent publication[6].

In all simulations the system was coupled to a constant temperature bath[2] with a relaxation time $\tau_T$ of 1.0 ps. The time step used in the simulation was 20 femtosecond[7]. In our simulations the neighbor-list was updated every 10 simulation steps. In analogy to other studies done with the MARTINI model, the time scales quoted in this work were scaled by a factor of four to correct for the four times faster diffusion rates of water and lipids found in the coarse grained model[5], with respect to reality. These corrected time scales, however, remain an approximate.

*The vesicle.* The vesicle used in this study was formed by spontaneous aggregation of the lipid components within the MFFA boundary set-up[1], as follows. We randomly inserted 1,250 di$C_{16}$-PC, 730 di$C_{18:2}$-PC, and 834 cholesterol molecules in a sphere with a 12.5 nm radius, respecting the excluded volume of each bead. The remaining volume of the shell was subsequently filled with CG water beads. In total, 49003 CG water beads were added. The system was initially run at a temperature of 323 K. Aided by the molding effect of the spherical boundary, rapid formation of a vesicle was observed within ≈100 ns.

*Compression of the vesicle.* In our simulations the vesicle was placed in an periodic simulation box of 24x24x24 nm. We applied two different methods of uni-axially compressing the vesicle: (i) Compression with its own periodic imagine. The latter was achieved by semi-isotropically coupling the pressure in the XY-plane to a reference pressure of 1 bar while coupling the pressure in the Z-dimension to 8 bar. A weak coupling scheme[2] with a relaxation time of $\tau_P$ of 0.5 ps was used. (ii) Compression between two repulsive planes. Here, an repulsive harmonic potential with an force constant of 50 KJ $mol^{-1}$ $nm^{-2}$ was used to compress the vesicle along the Z-dimension within a predefined offset. This potential only acted on the C-beads of both di$C_{16}$-PC and di$C_{18:2}$-PC (These lipids bare the same topology on the CG-level). The latter method assures that the lipid headgroups remain hydrated under compression. Similar methods have also been applied to estimate the free energy of hydrophilic membrane pores[3].

[1] H. J. Risselada, A. E. Mark, and S. J. Marrink, J. Chem. Phys. B **112**, 7438 (2008).
[2] H. J. C. Berendsen, J. P. M. Postma, W. F. van Gunsteren, A. Di Nola, and J. R. Haak, J. Chem. Phys. **81**, 3684 (1984).
[3] T. V. Tolpekina, W. K. den Otter, and W. J. Briels, J. Chem. Phys. **121**, 12060 (2004).
[4] B. Hess, C. Kutzner, D. Van Der Spoel, and E. Lindahl, J. Chem. Theory Comput. **4**, 435 (2008).
[5] S. J. Marrink, H. J. Risselada, S. Yefimov, D. P. Tieleman, and A. H. de Vries, J. Phys. Chem. B **111**, 7812 (2007).
[6] H. J. Risselada and S. J. Marrink, PNAS **105**, 17367 (2008).
[7] S. Marrink, X. Periole, D. P. Tieleman, and A. H. de Vries, Phys. Chem. Chem. Phys. **12**, 2257 (2010).

## MODEL: FREE ENERGY OF THE COMPRESSED VESICLE AND ASSUMPTIONS

The free-energy functional, $\Phi$, of the mixed vesicle takes the form

$$\begin{aligned}\Phi &= \sum_{\alpha\in\{\mathrm{lo,ld}\}}\int_{\Omega_\alpha}\mathrm{d}^2S\left(\frac{\kappa_{\mathrm{b},\alpha}}{2}[2H]^2+\bar{\kappa}_{\mathrm{b},\alpha}K+\frac{\kappa_{\mathrm{a},\alpha}}{2}\left[\frac{\sigma_\alpha}{\sigma_{\mathrm{o},\alpha}}-1\right]^2\right)+\int_{\partial\Omega}\mathrm{d}l\;\lambda\\ &+\sum_{\alpha\in\{\mathrm{lo,ld}\}}\Sigma_\alpha\left[\int_{\Omega_\alpha}\mathrm{d}^2S\;\frac{\sigma_\alpha}{\sigma_{\mathrm{o},\alpha}}-\bar{\varphi}_{\mathrm{o},\alpha}S_{\mathrm{o}}\right]-p(V-V_{\mathrm{o}})-F(2R-D)\end{aligned}\tag{1}$$

where the sum over $\alpha$ is comprised of the liquid-ordered and the liquid-disordered domains. $\Omega_\alpha$ denotes the area of a domain. $\kappa_{\mathrm{b},\alpha}$, $\bar{\kappa}_{\mathrm{b},\alpha}$, $\kappa_{\mathrm{a},\alpha}$ are the bending rigidity, Gaussian rigidity, and area compressibility of domain, $\alpha$. $\sigma_\alpha$ characterizes the lateral density in the domain, $\alpha$, and $\sigma_{\mathrm{o},\alpha}$ is the reference value in the tensionless state. $\partial\Omega$ is the domain boundary and $\lambda$ the concomitant line tension. The Lagrange multipliers $p$, $F$, and $\Sigma_\alpha$ enforce the constraint on the enclosed volume, the distance, $D$, between the flat contact zones and the number of molecules in the two domains. $\bar{\varphi}_{\mathrm{o}}$ denotes the area fraction of the domain, $\alpha$, on the tensionless vesicle. $\bar{\varphi}_{\mathrm{o}}\equiv\bar{\varphi}_{\mathrm{o,lo}}=1-\bar{\varphi}_{\mathrm{o,ld}}$.

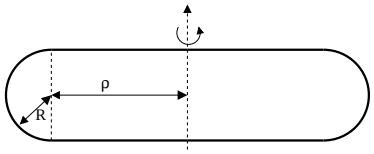


Figure 1: Geometry of the system considered in this letter. Compression of the vesicle along one dimension results in a barrel shape with half the thickness $r$ and length $\rho$.

In order to make progress, the following approximations and assumptions are made:

- Motivated by the observed structural changes we assume that the bending rigidity and area compressibility of the liquid-ordered domain depends on curvature in the following way

$$\kappa_{\mathrm{b,lo}} = \kappa_{\mathrm{b,lo,o}}\left(1-[dH]^2\right)\tag{2}$$

$$\kappa_{\mathrm{a,lo}} = \kappa_{\mathrm{a,lo,o}}\left(1-[dH]^2\right)\tag{3}$$

  where $d$ is a constant with dimension length, and it is expected to be on the order of the bilayer thickness. The dependence of all other material constants on curvature or tension is neglected.

- In principle, the shape of the uniaxially compressed vesicle is obtained by minimizing the free-energy functional. In the following we assume that the geometry of the vesicle is barrel-shaped (see below). This is a good approximation for a strongly squeezed vesicle, $\rho\gg R$, because the stretching contribution of the free energy is much larger than the bending one. We minimize the geometry with respect to the two variational parameters, $R$ and $\rho$.

- In the strongly compressed limit, the Gaussian curvature is small. Lacking knowledge of the Gaussian rigidity of the two phases, we ignore Gaussian contribution in the following. In any case, we do not expect this contribution would qualitatively change the results.

- We do not consider the density of the two apposing monolayers individually, which leads to a difference-area contribution to the free energy upon bending. The fast flip-flop of cholesterol in the liquid-disordered phase and the exchange of cholesterol between the domains partially mitigates this effect.

- We neglect the contribution associated with the line tensions, $\lambda$. The line tension prefers the minority domain to be placed on the curved part of the vesicle because this location minimizes the length of the domain boundary for a given domain area. This effect leads to budding of minority domains from planar membranes provided that the lateral extent of the domain is larger than the invagination length, $\kappa_{\mathrm{b}}/\lambda$. In our simulation, however, the lo domain is the majority component with area fraction, $\bar{\varphi}_{\mathrm{o}}\approx 0.64$. Moreover, using the values $\kappa_{\mathrm{b,lo}}\approx 4\cdot 10^{-19}$ J $\approx 100\,k_BT$ and $\lambda\approx 3.5$ pN we find that the concomitant length scale, $\kappa_{\mathrm{b}}/\lambda = 114$ nm, exceeds the vesicle

size. Moreover, the observation of *two* separated liquid-disordered domains suggests that minimizing the line tension is not the guiding principle dictating the morphology. Additionally, line-tension effects cannot explain why the domain sorting switches from reverse to normal upon reducing the enclosed volume but without altering membrane composition or vesicle geometry.

- In the numerical calculations, we assume that the entire liquid-ordered domain is placed on the curved rim of the barrel-shaped vesicle.

## GEOMETRY: BARREL SHAPE OF A MIXED VESICLE

Initially the shape of the tensionless vesicle is spherical with radius, $R_\mathrm{o}$, volume $V_\mathrm{o} = 4\pi R_\mathrm{o}^3/3$ and surface area, $S_\mathrm{o} = 4\pi R_\mathrm{o}^2$. In the uniaxially compressed state, the radius of the flat contact zone is denoted by $\rho$ and the distance between the two flat contact zones is $2R$. The special case, $\rho = 0$ and $R = R_\mathrm{o}$, corresponds to a spherical vesicle.

For the volume and the surface area of the barrel-shaped vesicle the following, approximate formulas hold:

$$\begin{aligned} V &= \pi\rho^2 \cdot 2R + \frac{\pi R^2}{2} \cdot 2\pi(\rho + \epsilon R) \qquad \text{with} \qquad 0 \le \epsilon \le 1 && (4)\\ &\approx \frac{4\pi}{3}R^3 + \pi^2 R^2\rho + 2\pi R\rho^2 \qquad \text{choosing} \qquad \epsilon = \frac{4}{3\pi} \qquad \text{fixed} && (5)\\ S &= 2\pi\rho^2 + \pi R \cdot 2\pi(\rho + \epsilon' R) \qquad \text{with} \qquad 0 \le \epsilon' \le 1 && (6)\\ &\approx 4\pi R^2 + 2\pi^2 R\rho + 2\pi\rho^2 \qquad \text{choosing} \qquad \epsilon' = \frac{2}{\pi} \qquad \text{fixed} && (7)\\ & && (8) \end{aligned}$$

They reproduce the correct forms in the spherical case and also in the strongly compressed limit, $\rho \gg R$.

Of course, $\int \mathrm{d}^2S\, K = 4\pi$ is an invariant, i.e., it does not depend on the shape or size of the vesicle. The mean and Gaussian curvature of the curved rim of the vesicle are approximately

$$K \approx \frac{1}{R} \cdot \frac{1}{R + \frac{\pi}{2}\rho} \tag{9}$$

$$H \approx \frac{1}{2}\left(\frac{1}{R} + \frac{1}{R + \frac{\pi}{2}\rho}\right) \tag{10}$$

where the approximate does obey the constraint for the invariant.

These assumptions lead to the following approximation of the free-energy functional

$$\begin{aligned} \Phi[\bar\varphi, \tilde\sigma_\mathrm{lo}, \tilde\sigma_\mathrm{ld}, \tilde\sigma'_\mathrm{ld}, \rho, R] \;=\; & \frac{\kappa_\mathrm{b,lo}(H)}{2}\bar\varphi S\,[2H]^2 + \frac{\kappa_\mathrm{b,ld}(H)}{2}\left([1-\bar\varphi]S - 2\pi\rho^2\right)[2H]^2 \\ & + \frac{\kappa_\mathrm{a,lo}(H)}{2}\bar\varphi S\,[\tilde\sigma_\mathrm{lo} - 1]^2 + \frac{\kappa_\mathrm{a,ld}(H)}{2}\left([1-\bar\varphi]S - 2\pi\rho^2\right)[\tilde\sigma_\mathrm{ld} - 1]^2 + \frac{\kappa_\mathrm{a,ld}(0)}{2}2\pi\rho^2\,[\tilde\sigma'_\mathrm{ld} - 1]^2 \\ & + \Sigma_\mathrm{lo}\left[\bar\varphi S\tilde\sigma_\mathrm{lo} - \bar\varphi_\mathrm{o}S_\mathrm{o}\right] + \Sigma_\mathrm{ld}\left[\left([1-\bar\varphi]S - 2\pi\rho^2\right)\tilde\sigma_\mathrm{ld} + 2\pi\rho^2\tilde\sigma'_\mathrm{ld} - (1-\bar\varphi_\mathrm{o})S_\mathrm{o}\right] \\ & - p(V - V_\mathrm{o}) - F(2R - D) \end{aligned} \tag{11}$$

where $\bar\varphi S$ denotes the area of the liquid-ordered domain (which is entirely located on the curved rim) and $S - 2\pi\rho^2 - \bar\varphi S > 0$ denotes the area of the liquid-disordered domain on the curved rim of the vesicle. $\tilde\sigma_\mathrm{ld}$ and $\sigma'_\mathrm{ld}$ denote the density of the liquid-disordered phase on the curved rim and the flat contact zone, respectively. $\tilde\sigma_\mathrm{lo} = \frac{\sigma_\mathrm{lo}}{\sigma_\mathrm{o,lo}}$, $\tilde\sigma_\mathrm{ld} = \frac{\sigma_\mathrm{ld}}{\sigma_\mathrm{o,ld}}$, and $\tilde\sigma'_\mathrm{ld} = \frac{\sigma'_\mathrm{ld}}{\sigma_\mathrm{o,ld}}$.

## MINIMIZING THE FREE-ENERGY FUNCTIONAL

Equations that constrain the geometry:

$$R = \frac{D}{2} \tag{12}$$

$$\text{solve} \qquad V(R,\rho) - V_\mathrm{o} = \frac{4\pi}{3}R^3 + \pi^2 R^2\rho + 2\pi R\rho^2 - V_\mathrm{o} = 0 \qquad \text{for } \rho(D) \tag{13}$$

$$\Rightarrow \qquad S = 4\pi R^2 + 2\pi^2 R\rho + 2\pi\rho^2 \tag{14}$$

$$H = \frac{1}{2}\left(\frac{1}{R} + \frac{1}{R + \frac{\pi}{2}\rho}\right) \qquad \text{and} \qquad K = 0 \tag{15}$$

Equations that determine $\bar{\phi}, \tilde{\sigma}_\mathrm{lo}, \tilde{\sigma}_\mathrm{ld}, \tilde{\sigma}'_\mathrm{ld}, \Sigma_\mathrm{lo}, \Sigma_\mathrm{ld}$

$$\frac{\partial\Phi}{\partial\bar{\varphi}} = \frac{\kappa_{\mathrm{b,lo}}}{2}S[2H]^2 - \frac{\kappa_{\mathrm{b,ld}}}{2}S[2H]^2 + \frac{\kappa_{\mathrm{a,lo}}}{2}S\left[\tilde{\sigma}_\mathrm{lo} - 1\right]^2 - \frac{\kappa_{\mathrm{a,ld}}}{2}S\left[\tilde{\sigma}_\mathrm{ld} - 1\right]^2 + \Sigma_\mathrm{lo}S\tilde{\sigma}_\mathrm{lo} - \Sigma_\mathrm{ld}S\tilde{\sigma}_\mathrm{ld} \stackrel{!}{=} 0 \tag{16}$$

$$\Rightarrow \qquad 0 = \frac{\kappa_{\mathrm{b,lo}}(H)}{2}[2H]^2 - \frac{\kappa_{\mathrm{b,ld}}(H)}{2}[2H]^2 + \frac{\kappa_{\mathrm{a,lo}}(H)}{2}\left[\tilde{\sigma}_\mathrm{lo} - 1\right]^2 - \frac{\kappa_{\mathrm{a,ld}}(H)}{2}\left[\tilde{\sigma}_\mathrm{ld} - 1\right]^2 + \Sigma_\mathrm{lo}\tilde{\sigma}_\mathrm{lo} - \Sigma_\mathrm{ld}\tilde{\sigma}_\mathrm{ld} \tag{17}$$

$$\frac{\partial\Phi}{\partial\tilde{\sigma}_\mathrm{lo}} = \kappa_{\mathrm{a,lo}}\bar{\varphi}S\left[\tilde{\sigma}_\mathrm{lo} - 1\right] + \Sigma_\mathrm{lo}\bar{\varphi}S \stackrel{!}{=} 0 \tag{18}$$

$$\Rightarrow \qquad \Sigma_\mathrm{lo} = -\kappa_{\mathrm{a,lo}}\left[\tilde{\sigma}_\mathrm{lo} - 1\right] \tag{19}$$

$$\frac{\partial\Phi}{\partial\tilde{\sigma}_\mathrm{ld}} = \kappa_{\mathrm{a,ld}}\left([1-\bar{\varphi}]S - 2\pi\rho^2\right)\left[\tilde{\sigma}_\mathrm{ld} - 1\right] + \Sigma_\mathrm{ld}\left([1-\bar{\varphi}]S - 2\pi\rho^2\right) \stackrel{!}{=} 0 \tag{20}$$

$$\Rightarrow \qquad \Sigma_\mathrm{ld} = -\kappa_{\mathrm{a,ld}}(H)\left[\tilde{\sigma}_\mathrm{ld} - 1\right] \tag{21}$$

$$\frac{\partial\Phi}{\partial\tilde{\sigma}'_\mathrm{ld}} = \kappa_{\mathrm{a,ld}}2\pi\rho^2\left[\tilde{\sigma}'_\mathrm{ld} - 1\right] + \Sigma_\mathrm{ld}2\pi\rho^2 \stackrel{!}{=} 0 \tag{22}$$

$$\Rightarrow \qquad \Sigma_\mathrm{ld} = -\kappa_{\mathrm{a,ld}}(0)\left[\tilde{\sigma}'_\mathrm{ld} - 1\right] \tag{23}$$

$$\bar{\varphi}_\mathrm{o}S_\mathrm{o} = \bar{\varphi}S\tilde{\sigma}_\mathrm{lo} \tag{24}$$

$$(1-\bar{\varphi}_\mathrm{o})S_\mathrm{o} = \left([1-\bar{\varphi}]S - 2\pi\rho^2\right)\tilde{\sigma}_\mathrm{ld} + 2\pi\rho^2\tilde{\sigma}'_\mathrm{ld} \tag{25}$$

The remaining two conditions, $\frac{\partial\Phi}{\partial\rho} = \frac{\partial\Phi}{\partial R} \stackrel{!}{=} 0$, dictate the strength of the two Lagrange multipliers $p$ and $F$. They are not required for the following.

The free energy of the vesicle is given by substituting the saddle-point values back into the free-energy functional

$$\begin{aligned}\Phi_\mathrm{min} = {} & \frac{\kappa_{\mathrm{b,lo}}(H)}{2}\bar{\varphi}S\left[2H\right]^2 + \frac{\kappa_{\mathrm{b,ld}}(H)}{2}\left([1-\bar{\varphi}]S - 2\pi\rho^2\right)\left[2H\right]^2 \\ & + \frac{\kappa_{\mathrm{a,lo}}(H)}{2}\bar{\varphi}S\left[\tilde{\sigma}_\mathrm{lo} - 1\right]^2 + \frac{\kappa_{\mathrm{a,ld}}(H)}{2}\left([1-\bar{\varphi}]S - 2\pi\rho^2\right)\left[\tilde{\sigma}_\mathrm{ld} - 1\right]^2 + \frac{\kappa_{\mathrm{a,ld}}(0)}{2}2\pi\rho^2\left[\tilde{\sigma}'_\mathrm{ld} - 1\right]^2\end{aligned} \tag{26}$$

It is comprised of a bending and a stretching contribution.

The free energy of the normal arrangement is obtained by reversing the material constants of the liquid-ordered and liquid-disordered phase. In case of normal ordering, the liquid-ordered domain is simultaneously located both on the flat contact zone and the curved rim.

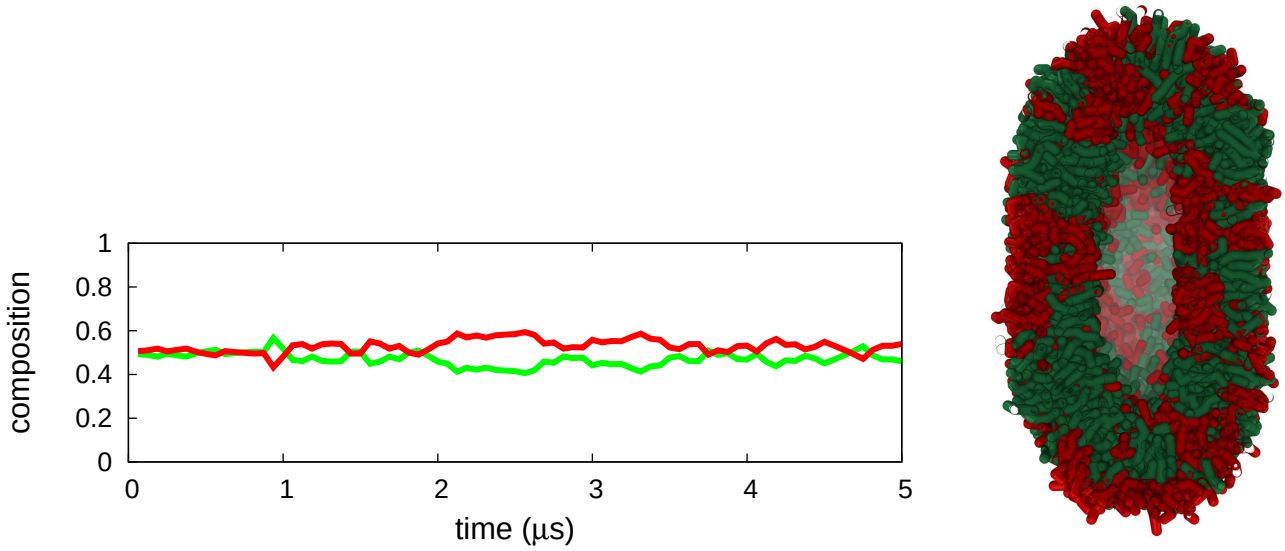


Figure 2: Lipid sorting in a 1:1 $diC_{16}$-PC:$diC_{18:2}$-PC binary mixed vesicle under uni-axially compression at 295 K ($R$ =6 nm, $\Delta p > 0$ bar, T < $T_c$). (Left figure) Lipid composition in the flat contact region versus time. No significant sorting is observed during the 5$\mu$s of simulation. (Right figure) Snapshot of the system at 5$\mu$s. Color scheme: saturated $diC_{16}$-PC is shown in green and unsaturated $diC_{18:2}$-PC in red.

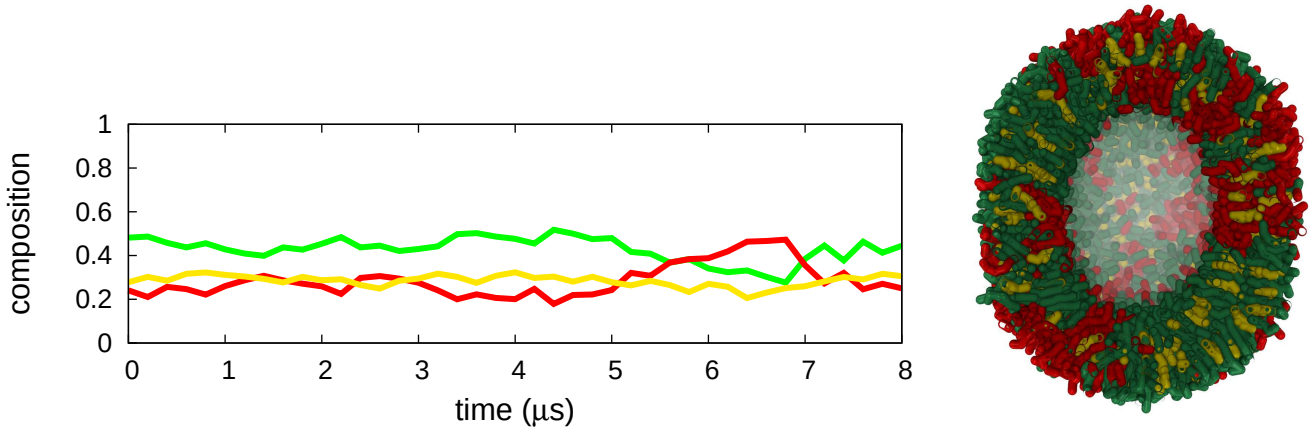


Figure 3: Lipid sorting in a ternary mixed vesicle under lower uni-axially compression at 295 K ($R$ =9 nm, $\Delta p > 0$ bar, T < $T_c$). (Left figure) Lipid composition in the flat contact region versus time. No significant curvature mediated sorting is observed during the 8$\mu$s of simulation. (Right figure) Snapshot of the system at 8$\mu$s. The snapshot reveals the presence of lo domains that are randomly distributed over the compressed vesicle. When the coupling between curvature and bending rigidity and coupling between curvature and area compressibility equally contribute to the free energy of sorting the domains are expected to lose their curvature preference. Color scheme: saturated $diC_{16}$-PC is shown in green and unsaturated $diC_{18:2}$-PC in red, cholesterol in yellow.